

Control of resputtering in biased CoCrPt–SiO₂ media to enhance grain decoupling and grain size distribution

Hwan-Soo Lee,^{a)} Vickie W. Guo, Jian-Gang Zhu, and David E. Laughlin

Data Storage Systems Center, Department of Electrical and Computer Engineering, Carnegie Mellon University, Pittsburgh, Pennsylvania 15213, USA

(Presented on 8 November 2007; received 13 September 2007; accepted 25 January 2008; published online 18 March 2008)

A CoCrPt–SiO₂ magnetic layer was investigated as functions of argon pressure and substrate bias voltage. Use of these two parameters provided fine tuning of the average kinetic energy of incoming Ar⁺, which causes resputtering and, consequently, influences adatom mobility during film growth. Biasing and high Ar pressure resulted in a significant improvement in grain decoupling and grain size distribution in the films. Furthermore, resputtering of the metal and oxide species from the growing CoCrPt–SiO₂ film was interpreted in terms of the surface adhesion energy of the species on the metal Ru underlayer. © 2008 American Institute of Physics. [DOI: 10.1063/1.2845030]

I. INTRODUCTION

Oxide-containing granular (or oxide composite) media have been shown to produce fine grains that are decoupled by oxide at the grain boundaries, leading to low noise performance in disk drive media.^{1,2} In Co-alloy thin film media, Ru/Ru-oxide layer,³ Ru–SiO₂ underlayer,⁴ and oxide seed layer with low surface energy⁵ have been suggested as methods to attain better intergranular exchange decoupling in the magnetic layer.

Previously, biasing was found to be very effective in reducing intergranular exchange coupling in the films^{6,7} but it had an effect of reducing the total amount of oxide in the growing CoCrPt–SiO₂ films even with a small bias voltage due to *resputtering* and promoting the growth of larger Co-alloy grains. These growth characteristics were interpreted to arise mainly from weak surface bonding of molecules to the nontextured growth and their strong bonding to the textured growth.

In this study, argon sputtering pressure (P_{Ar}) and bias voltage (V_B) during deposition were used to achieve well-separated grains and enhance the grain size distribution while pertaining to small grains. The sputtering pressure and bias voltage are thought to provide fine tuning of the average kinetic energy of incoming Ar⁺ which strikes the substrate and causes resputtering. We specifically examine the effects of P_{Ar} and V_B on the morphology of the CoCrPt–SiO₂ composite films and discuss the role of these two parameters by thinking in terms of the surface adhesion energy of SiO₂ on the Ru underlayer.

II. EXPERIMENTAL

CoCrPt–SiO₂ thin films were deposited on Si substrate/Ta (5 nm)/Ru (30–40 nm) underlayers. The CoCrPt–SiO₂ films were made under different argon sputtering and bias conditions without intentional substrate heating. Deposition of the magnetic layer was carried out at about a

2.3 W/cm² (=100 W) sputtering power (SP) density unless stated otherwise. A CoCr alloy target with bonded Pt and SiO₂ chips was used for magnetic film preparation. All underlayers were deposited under a fixed set of conditions. Care was taken to ensure that no significant temperature increase occurred during deposition, even when the bias was applied. The surface roughness was measured using an atomic force microscopy (AFM). The typical measurement area was $2 \times 2 \mu\text{m}^2$. The film composition was determined by energy dispersive x-ray fluorescence analysis. Film textures and microstructures were characterized by an x-ray diffractometer (Philips X'pert Pro with x-ray lens) using Cu $K\alpha$ radiation and by a JEOL JEM-2010 transmission electron microscope (TEM) operating at 200 kV.

III. RESULTS AND DISCUSSION

Figure 1 shows the effect of P_{Ar} on the grain morphology of the CoCrPt–SiO₂ films. A substrate bias of -120 V was applied for this investigation. As previously reported, at an argon pressure of 10 mTorr, a large reduction in SiO₂ content due to resputtering is seen [see the inset (unbiased case) in Fig. 1(a)]. The very distinct oxide removal due to preferential resputtering was interpreted to arise largely from weak surface bonding to the growing films for nontextured growth of SiO₂ on the metal (Ru) underlayer.⁷

As P_{Ar} was increased, biasing removed less amount of the SiO₂ in the growing films and a much better defined SiO₂

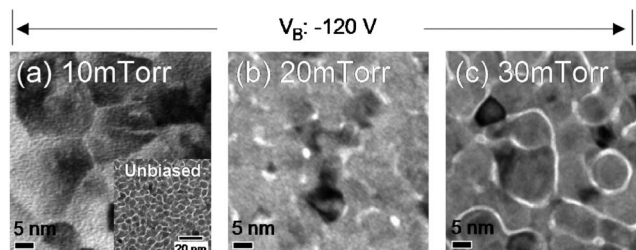


FIG. 1. Plan-view TEM micrographs of biased CoCrPt–SiO₂ media for different Ar pressures. The bias voltage applied during depositing the magnetic layer was -120 V.

^{a)}Electronic mail: hwansoo@cmu.edu.

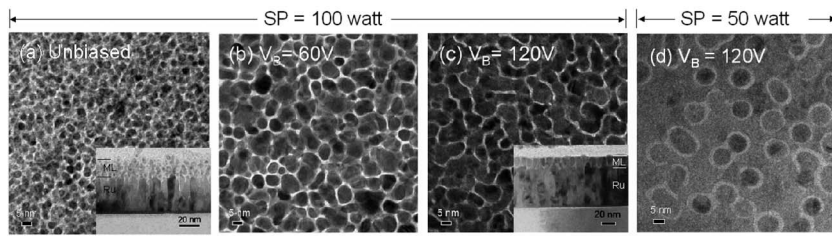


FIG. 2. Plan-view TEM micrographs of CoCrPt-SiO₂ media deposited as a function of substrate bias (V_B): (a) unbiased, (b) $V_B = -60$ V, and [(c) and (d)] $V_B = -120$ V. The SP is 100 W for (a)-(c) whereas the SP is 50 W for (d). The argon sputtering pressure (P_{Ar}) for the samples was 40 mTorr. The insets correspond to cross-sectional TEM micrographs where ML is the magnetic layer.

on the thicker boundary was observed. We attribute this to lower mean energy of the Ar⁺ striking the substrate due to greater collision losses at higher P_{Ar} .

Additionally, at an argon pressure of 20 mTorr, it is interesting to note that the oxide phase (SiO₂), which corresponds to the white contrast, is mostly observed at triple or quadruple junctions of grains. This suggests that as films are sputter deposited, those sites are more likely to act as a nucleation site due to lower interfacial energy when SiO₂ molecules come down onto the substrate and SiO₂ at the junctions, where it is easily coordinated with other SiO₂ molecules, has a lower resputter yield than SiO₂ molecules at other places.

In Fig. 2, plan-view TEM micrographs of the CoCrPt-SiO₂ films are shown as a function of bias voltage. An SP of 50 W that corresponds to about 1.1 W/cm² SP density was used for the sample in Fig. 2(d) whereas an SP of 100 W (=2.3 W/cm²) was employed for the others. The samples were all deposited at an argon pressure of 40 mTorr. The grain size for the unbiased case is less than 5 nm. As the films are bias sputtered, grains become better isolated and grow being columnar, though substantially larger than in the unbiased case.

The film morphology through thickness direction is notable. The insets in Figs. 2(a) and 2(c) are the corresponding cross-sectional TEM images, respectively. For the unbiased CoCrPt+SiO₂ films, spherically shaped CoCrPt particles are seen. The oxide acts as a matrix where the metal particles are embedded in the through thickness direction. This resulted in the magnetic layer being random in its crystalline orientation and gave rise to a very low H_c of less than 100 Oe. In contrast, the biased CoCrPt+SiO₂ film appears to be highly columnar at the thickness dimension.

It is also important to note that the biased CoCrPt+SiO₂ films exhibited a much smoother surface (compare the insets in Fig. 2). Biasing is known to have an effect of planarizing the topography of the surface.⁸ In support of the above cross-sectional images, the measured rms of the surface roughness using AFM (not included) was shown to be 1.01 nm (unbiased) and 0.64 nm (biased), respectively.

In Fig. 2(d), SP is shown to have an important bearing on determining the grain morphology as well. A larger visual grain size of about 8–10 nm for this specimen is seen. We speculate that the lower SP allows the SiO₂ phase to have a longer time to segregate and reach equilibrium before burial under a circumstance where the CoCrPt and SiO₂ repeatedly nucleate through the film thickness to yield columnar grains. However, the segregation process appears to be less uniform, varying the thickness of grain boundaries. Some grains indicate clearly defined thick grain boundaries but some show

much thinner boundaries. More uniform nucleation events of the SiO₂ phase on the Ru underlayer surface seem to be necessary as the CoCrPt+SiO₂ is initially deposited on the underlayer template. Nonetheless, a better grain isolation is evident for the biased samples as higher biasing and lower SP were employed.

More importantly, the grain size distribution can be influenced with biasing as well. As shown in Fig. 3, the grain size distribution in the biased CoCrPt-SiO₂ films was appreciably narrower at higher substrate bias. The unbiased case was excluded for this investigation since grains are spherically shaped in the through direction instead of being columnar in its growth morphology. The mean grain diameter (GD) and its standard deviation (σ) of the higher biasing case (-120 V) are 6.1 and 2.4 nm while those of the biased media of -60 V are 5.3 and 4.6 nm, respectively. The number of grains taken for the analysis was about 150-200 and the thickness of grain boundaries was not included in the estimation. The average GD and σ was determined by fitting the histogram of grain diameters with a Gaussian function. Higher bias slightly enhanced GD and, more noticeably, reduced σ of the magnetic layer, presumably due to the fact that bias sputtering increases adatom mobility during film growth and, consequently, influences nucleation density.⁹

In Fig. 4 an x-ray diffraction (XRD) spectrum of the biased media is shown. The biased CoCrPt+SiO₂ medium has a CoCrPt (00.2) texture. Similarly, use of substrate bias for CoCrTa layer was reported to help the crystalline structure improved, exhibiting highly *c*-axis textured films.¹⁰ In the inset, the corresponding magnetic properties of the biased medium indicate a coercivity H_c of 2.15 kOe, a squareness of 0.94, and a sheared slope, implying magnetic isolation owing to the well-segregated microstructure. The rather low H_c is thought to be due to not optimized Pt and Cr contents in the films. The Pt and Cr contents for the media were 25 and 16 at. %, respectively. Piramanayagam *et al.* indicated that effect of bias voltage was detrimental to the structural and magnetic properties when applied for the CoCrPt

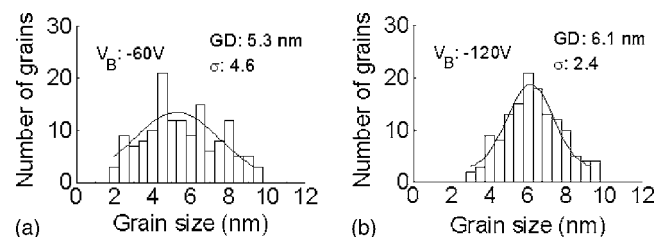


FIG. 3. Mean GD and its standard distribution (σ) are measured by image analyzing process for the samples shown in Fig. 2. Solid curves are fitted using Gaussian distribution function: (a) $V_B = -60$ V and (b) $V_B = -120$ V.

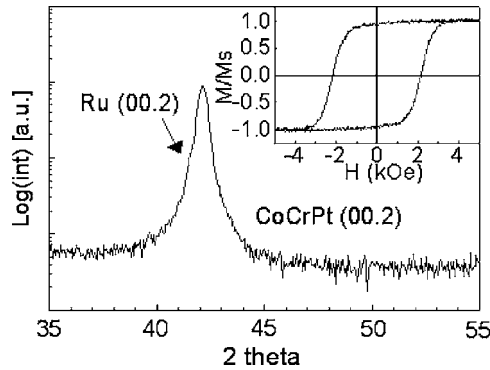


FIG. 4. XRD spectrum of the bias-sputtered CoCrPt-SiO₂ film deposited on substrate-Ta/Ru underlayer template, indicating to be *c* axis textured. The inset corresponds to hysteresis loop.

+SiO₂ recording layer.¹¹ This was attributed to the oxide removal from the recording layer, which would form a continuous structure and influence the exchange decoupling. However, a control in the oxide resputtering was not further exploited in their study, which makes a direct comparison difficult.

The effects of argon sputtering pressure and substrate bias on deposition rate of the CoCrPt-SiO₂ films are also worth noting (not shown). The deposition rate at an argon pressure of 10 mTorr decreased from 9 to 5 nm/min as the substrate bias was changed from 0 to -120 V, whereas the deposition rate at an argon pressure of 40 mTorr decreased from 12.3 to 7.5 nm/min. The CoCrPt-SiO₂ deposition rate decreased as V_B increased due to resputtering whereas higher P_{Ar} increased the deposition rate and the oxide content in the films. The estimated volume fraction of the metal (CoCrPt) and oxide (SiO₂) phases for the CoCrPt-SiO₂ media with respect to argon pressure also revealed that SiO₂ molecules on the Ru are more susceptible to resputtering at lower argon pressure. In order to measure the volume fraction, a simple estimate was made of an assumption for cylindrical grains for the biased media, which seems to be reasonable since columnar growth in the biased films was observed.

Figure 5 shows in outline how resputtering can be performed for different argon sputtering pressures by thinking in terms of the distribution of surface adhesion energy for the SiO₂ or metal (CoCrPt) species on the metal Ru underlayer.

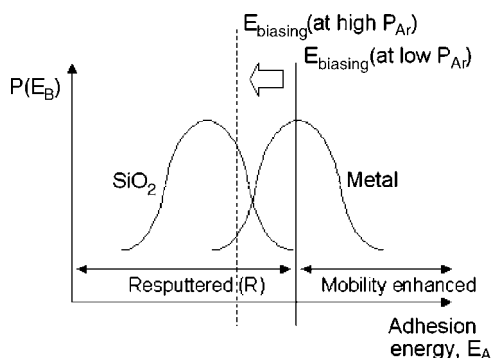


FIG. 5. A schematic illustration of resputtering in terms of surface adhesion energy of the SiO₂ on the metal (Ru) underlayer for different P_{Ar} .

The CoCrPt, which was heteroepitaxially grown on the Ru layer, appears to strongly bond to the Ru underlayer. On the other hand, adhesion energy for the case of SiO₂ on Ru underlayer, which was grown nonepitaxially, is likely to be smaller since biasing removed larger amount of the SiO₂ in the growing films (presumably less than 1 eV). Consistent with this, adhesion energy calculated between Cu and SiO₂ substrates¹² was shown to be smaller than 1 eV while the reported interface adhesion energies for metal on metal are typically several eV, which points to the nature of the interfacial bonding (i.e., metal/metal > metal/oxide).¹³

Figure 5 illustrates that energy of biasing (E_B) is reduced due to collision losses and shifts to the left as argon sputtering pressure is increased (indicated by the dotted line). Higher argon sputtering pressure increases the amount of scattering of argon (Ar⁺) and, as a result, leads the species to be less etched away from the growing film during bias sputtering. In support of this, a lower resputtering yield for the both species was observed.

Finally, we summarize that bias sputtering can lead to either an increase or decrease in the content of the species from the growing films, depending on their surface adhesion characteristics which in turn control their resputtering.

IV. CONCLUSIONS

The relationship between resputtering in biased CoCrPt-SiO₂ films and the corresponding grain morphology has been investigated. Understanding of resputtering and segregation process in terms of surface adhesion of SiO₂ on metal underlayer leads to isolated magnetic grains with smaller grain size distribution. Within the parameter range of this investigation, higher biasing (-120 V) and higher argon pressure (40 mTorr) appear to display desirable oxide composite media properties, which can lead to low media noise. Such features of bias sputtering, with its various advantages, can be greatly useful to attain oxide composite high density recording media.

¹T. Oikawa, M. Nakamura, H. Uwazumi, T. Shimatsu, H. Muraoka, and Y. Nakamura, *IEEE Trans. Magn.* **38**, 1976 (2002).

²H. Uwazumi, K. Enomoto, Y. Sakai, S. Takenoiri, T. Oikawa, and S. Watanabe, *IEEE Trans. Magn.* **39**, 1914 (2003).

³U. Kwon, R. Sinclair, E. M. T. Velu, S. Malhotra, and G. Bertero, *IEEE Trans. Magn.* **41**, 3193 (2005).

⁴I. Takekuma, R. Araki, M. Igarashi, H. Nemoto, I. Tamai, Y. Hirayama, and Y. Hosoe, *J. Appl. Phys.* **99**, 08E713 (2006).

⁵S. H. Kong, K. Mizuno, T. Okamoto, and S. Nakagawa, *J. Appl. Phys.* **93**, 6781 (2003).

⁶H.-S. Lee, J. A. Bain, and D. E. Laughlin, *J. Appl. Phys.* **99**, 08G910 (2006).

⁷H.-S. Lee, J. A. Bain, and D. E. Laughlin, *Appl. Phys. Lett.* **90**, 252511 (2007).

⁸D. T. C. Huo, M. F. Yan, C. P. Chang, and P. D. Foo, *J. Appl. Phys.* **69**, 6637 (1991).

⁹T. Yogi, T. A. Nguyen, S. E. Lambert, G. L. Gorman, and G. Castillo, *IEEE Trans. Magn.* **26**, 1578 (1990).

¹⁰K. Okimura and J. Oyanagi, *J. Vac. Sci. Technol. A* **23**, 39 (2005).

¹¹S. N. Piramanayagam, C. S. Mah, C. Y. Ong, J. Z. Shi, J. A. Dumaya, T. Onoue, and S. Ishibashi, *J. Appl. Phys.* **101**, 103914 (2007).

¹²K. Nagao, J. B. Neaton, and N. W. Ashcroft, *Phys. Rev. B* **68**, 125403 (2003).

¹³J. N. Andersen, O. Bjorneholm, A. Stenborg, A. Nilsson, C. Wigren, and N. Martensson, *J. Phys.: Condens. Matter* **1**, 7309 (1989).